Title

Emergence of a maximum soil flux under drought governs stomatal responsiveness to vapor pressure deficit over sub-daily and daily timescales.

Author list

Fulton E. Rockwell

Affiliations

Corresponding author and email

Fulton E. Rockwell, fulton.rockwell@gmail.com

Orcids: 0000-0002-2527-6033

Summary

The combination of drought and heat waves is known to have synergistic effects on mortality as plants experience both supply and demand-side water stress. Yet which of these most strongly down-regulates stomatal conductance remains at issue.

- Losses of soil hydraulic conductivity are modeled in a soil domain fed by a maximum water flux from a water table. Root uptake extracts water from the soil based on a two-node (root and leaf) plant model, with stomatal conductance a function of leaf water potential, and transpiration driven by vapor pressure deficit (VPD).

- The results of multi-day simulations reproduce published observations of near-perfect conservation of transpiration despite a doubling of VPD and show that the sensitivity of stomatal conductance to VPD depends on the ratio of total daily potential transpiration to the maximum soil flux. Osmotic adjustment to maintain open stomata to lower water potentials is shown to be ineffective for increasing carbon gain.

- Given estimates for the effective root to water table depth, use of a maximum soil water flux boundary condition could improve prediction of plant canopy responses to the twin stressors of drought and atmospheric aridity.

Keywords [plant drought response, vapor pressure deficit, soil hydraulics, heatwave, hydraulic limitation, stomatal conductance]

Table of word counts each section (I, MD, R, D). Num figs. Num Tables, num SI.

Total word count	7890	No. of Figures	7
Introduction	1557	No. of Tables	0
Model Description	1628	No. of Supporting Information files	4
Results	2334		
Discussion	2371		

Introduction

The dual role of stomata in admitting an inward flux of CO_2 while also preventing the desiccation of plant tissues has been recognized at least since Van Den Honert (1948), who proposed that stomata serve as the dominant resistance to water transport in the soil-plant-atmosphere continuum (Philip, 1966). While guard cells, as hydraulicly actuated valves, respond 'passively' to local water status, they are also decoupled from the local water potential of the epidermis by 'active' biochemistry (e.g., light activated ion pumping, ABA induced closure; (McAdam & Brodribb, 2016; Jezek & Blatt, 2017), with the result that the strategies and control points (e.g., local water potential, foliar versus root synthesized ABA) governing stomatal regulation itself remain uncertain (Tardieu & Simonneau, 1998; Buckley, 2005; McAdam & Brodribb, 2016; Jezek *et al.*, 2019; Carminati & Javaux, 2020). One important area of focus has been on the role of variable hydraulic resistances in the induction of stomatal closure in response to drying of the soil and atmosphere. Sperry et al. (1998) modeled water transport through a discretized soil-plant continuum, accounting for stress induced declines in both soil hydraulic conductivity and plant xylem conductivity, concluding that xylem vulnerability was likely to be the dominant dynamic factor contributing to stomatal regulation. Following a change in the scientific consensus on the degree to which plants cavitate and refill xylem conduits under diurnal water stress (Wheeler *et al.*, 2013; Torres-Ruiz *et al.*, 2015), Sperry & Love (2015) proposed a steady-state continuum model of the xylem in which incipient losses of xylem conductance, losses that if realized would ultimately lead to an asymptotic maximum *E*, serve as a set point for stomatal regulation. In this model, stomatal regulation of *E* emerges from the

hypothesis of an evolved coordination of xylem vulnerability and stomatal regulatory traits, rather than a mechanistic model of hydro-chemo-mechanical guard cell responses to local water potentials, such as Buckley (2005).

Carminati & Javaux (2020) took a similar approach to Sperry and Love (2015), but found that with their parameterization soil conductivity emerged as the likely factor limiting transpiration. Carminati and Javaux (2020) hypothesized that stomatal regulation evolved to avoid the "stress onset limit (SOL)," or the leaf water potential at which further declines drove only a small increase in the flux from the soil into the leaf. In addition to losses of hydraulic conductivity in the soil itself, root-soil contact has emerged as another source of variable resistance. Drying of root mucilage or root shrinkage with the onset of soil water stress could lead to an increase in air gaps between the soil and roots, with liquid flow across the contact zone increasingly replaced by relatively inefficient water vapor diffusion, creating a bottle neck (Carminati *et al.*, 2009, 2016; Rodriguez-Dominguez & Brodribb, 2020; Manandhar *et al.*, 2024).

Cowan (1965) developed a transient continuum model of the soil coupled to an ohmic model of a plant with constant xylem conductivity. In this model, the extreme non-linearity of the losses of soil hydraulic conductivity proximal to the root ultimately forced the leaf to its critical leaf water potential (at which stomata went from full open to full shut) each day, as bulk soil water and total transpiration declined, while overnight root water potential recovered to bulk soil water potential, even as the latter declined monotonically over the multiday model run (Fig. 11 in Cowan). In this and similar models, a critical leaf water potential for stomatal closure was defined that effectively served as a transition point from perfect anisohydry to perfect isohydry (Cowan, 1965; Hochberg *et al.*, 2018; Javaux & Carminati, 2021). All the models discussed so far emphasize supply limitations on transpiration, with Cowan (potential E) and Sperry and Love (loss function) taking different approaches to showing how variation in atmospheric demand pulls leaf water potential closer to the point where further reductions in 'upstream' (soil or stem xylem) conductivity cause further increases in E to vanish. Yet none of these studies incorporates stomatal conductance as a function of leaf water potential, the variable that sensitizes stomatal water balance to both soil supply and atmospheric demand.

The problem of partitioning changes in stomatal aperture between supply and demand limitation also arises in the modeling of canopy conductances to vapor pressure deficit (VPD). One

approach has been to model a maximum or reference value of canopy conductance as a function of soil moisture, then fitting a slope parameter that describes the erosion of conductance with increasing vapor pressure deficit (Oren *et al.*, 1999; Novick *et al.*, 2016). Using data from eddy flux sites, Novick *et al.* (2016) fitted ecosystem scale *VPD* responses to model the response of canopy conductance and transpiration to a hypothesized increase in atmospheric aridity with climate warming. This approach has attracted criticism, based on the observation that at the relevant spatial and temporal scales, soil moisture and *VPD* are not independent (Roderick *et al.*, 2015; Novick *et al.*, 2016; Berg & Sheffield, 2018). Yet, even at the instantaneous physiological scale of flux tower data, it is unclear, based on the above models, to what extent dynamic soil effects on leaf water potential that feed into control of stomatal conductance can be adequately captured by bulk soil moisture. If not, then apparent stomatal responses to *VPD* may be driven in part by dynamic soil losses in conductivity.

The current study explores the link between soil conductivity and *VPD* responses by modeling the 'heat wave' experiments of (Drake *et al.*, 2018), originally designed to capture the effect of *VPD* and temperature anomalies on canopy conductance, transpiration and assimilation. In this field experiment, eucalyptus trees (~ 6 m tall) were enclosed in single-tree 9 m tall chambers that allowed control of temperature and humidity as well as measurements of gas exchange (CO_2, H_2O). The goal of the experiment was to understand the physiological impact and response of pre-droughted trees to a heat wave ('Heat Wave' treatment), combining air temperature (daily peak 43-44°C) and *VPD* stress (daily peak 5-6 kPa), versus a Control subject to typical atmospheric conditions (daily peaks of 28-29 ^{o}C, 2-2.5 kPa). Motivation for the experiment can be derived from observations that the twin stressors of heat and drought are known to have synergistic mortality effects (Mitchell et al., 2014; Matusick et al., 2018).The trees subject to the Heat Wave treatment showed a remarkably tight stomatal response, with total daily transpiration (E_d) in the heat wave treatment showing no increase over the control despite a doubling of *VPD* (Fig. 2 in Drake *et al.*, 2018). Such perfect stomatal control maintaining constant daily *E* across both *VPD* levels and multiple days could not emerge simply from a linear (constant resistance) feedback of leaf water potential on stomatal aperture (Dewar 2002; Buckley 2003), as such feed-backs are expected to act only to limit an increase in *E* as *VPD* changes, not hold *E* constant. Strict stomatal control could have emerged from variable xylem or soil resistance, as in the steady-state Sperry and Love (2015) or Carminati and Javaux (2020) models described above,

yet xylem losses of conductivity in the Drake experiment may be eliminated as no evidence of loss of stem or leaf xylem conductance was found.

The absence of evidence for losses of plant hydraulic conductivity raises the question of whether losses of soil conductivity feeding into leaf water potential could explain such strict control of transpiration alone, or whether a separately parameterized *VPD* response, as might occur due to ABA (i.e., 'feed forward' responses in Parkhurst & Mott, 1990; McAdam & Brodribb, 2016) is required to fully capture the observed behavior of *E* in the Drake *et al.* (2018) experiment. While the approach of Cowan might serve to test this hypothesis, the stability of E_d across days implies that a re-charge of soil moisture and recovery in the variable resistance occurred overnight, incompatible with the initial fixed and monotonic decline of soil water content in that model. Specifying an implicitly infinite reservoir of fixed soil moisture between each root and its neighbor could provide the required water source, but while reasonable for a steady-state 'slice' of time in the Carminati and Javaux (2020), or Sperry *et al.* (1998) and Sperry and Love (2015) models, the ambiguity about the 'true' location of a non-depleting bulk soil reservoir over a time scale of days makes comparison of this model structure to data problematic.

In the physical experiment, irrigation was withheld from the enclosed plants, leaving ground water as the only possible source for recharging a diurnally drying soil domain. Incorporating a ground water source in the transient model framework of Cowan (1965) would be impractical due to a mismatch in scale and geometry. In that model, the steepest gradients in soil water content and potential are expected to occur over the mm scale in a cylindrical domain around an individual root, yet transport from the water table is most readily described using a one-dimensional cartesian frame over a scale of meters. Here we propose a resolution to these mismatches of geometry and scale and model the Drake *et al.* (2018) experiment to test whether this new approach can recover the observed conservation of total daily transpiration across different *VPD* levels. The model is then employed to further explore the uncoupling of *E* from *VPD* due to dynamic changes in soil hydraulic conductivity, including the effectiveness of osmotic adjustment to maintain carbon gain under drought.

Model Description

To overcome the geometrical mismatch created by trying to connect a source of water at some 1D depth to the outer boundary of the 2D soil cylinder around a root, both root uptake and the

source are further abstracted (Fig. **1**). The cylinder of soil around a representative root is replaced by an 'uptake plane' introduced at maximum rooting depth in the soil column. Though it may seem artificial relative to the soil cylinder, this representation is at least consistent with the typical SPAC representation of the above ground plant canopy as a plane of zero thickness for energy absorption and gas exchange. And even as the leaves at the very top of the canopy likely dominate the gas exchange of the entire canopy, the concept of a rooting plane captures the behavior of uptake being dominated by the roots in contact with the wettest soil region independent of rooting density (Dawson et al., 2020). Nevertheless, this abstraction comes at the cost of not capturing the extra 'geometrical resistance' created by the concentration of the flux as it approaches the root. Representing the root zone as a 'plane of uptake' then rests on the hypothesis that such geometrical effects are not required to capture the observed behavior of the physical experiment in the model, which will be true if dynamic losses of soil conductivity dominate the behavior.

To further address the length scale mismatch between the millimeter scale gradients in matric potential expected near the rooting surface and the meter scale distance from the rooting zone to the water table, a centimeter scale domain of interest is defined with a boundary condition that employs a 'maximum soil flux' concept to represent flow into the domain from the source (Supplemental Notes S**1**). Briefly, a maximum soil flux emerges from the extreme non-linearity of losses of soil hydraulic conductivity that occur with declines in soil moisture: as the potential of the evaporative soil surface goes to negative infinity, the flux pulled from the water table grows asymptotically to a maximum (Jury *et al.*, 1991). Physically, at the maximum flux the water column in the soil simply breaks as the surface pulls harder on the water column rather than permitting any increase in flow rate. The nice feature of this boundary condition is that it depends only on soil properties and the distance from the rooting plane (i.e., evaporative or uptake surface) to the water table, independent of the actual soil water content or matric potential at the boundary. This uncoupling of the inward flux and level of dryness at the boundary frees the model from having to solve for the gradients in potential that must exist over the meter-scale distance from the water table to the rooting plane. It also means that this maximum flux condition is appropriate both for steady state, and for the case that the dryness at the boundary is fluctuating diurnally.

To complete the modeling approach, uptake from the domain of interest (Fig. **1a**) occurs at a rooting plane that acts as the upper boundary of the domain. This flux of water out of the soil is driven by transpiration from a plant model featuring two nodes (root and leaf water potential) separated by a constant whole plant conductance (Supplemental Notes **S1**). The neglect of cavitation in the plant is justified by leaf and stem measurements in the supplemental Information of Drake *et al.* (2018) that show no reduction in hydraulic conductance occurred during the experiment. The neglect of plant capacitance follows Cowan's (1965) arguments that soil capacitance is expected to dominate the time scale of storage effects: as a result, flux out of the rooting plane is equivalent to the flux out of the leaf at every time step. As the trees in the physical experiment were in large chambers with well-stirred air, we expect that the aerodynamic canopy conductance was non-limiting and so total canopy conductance was close to stomatal conductance, and leaf temperature close to air temperature (*e.g.*, Fig. 4 in Drake et al 2018). In this isothermal well-mixed limit, transpiration can be expressed as the product of a potential evapo-transpiration rate (E_p) that carries the units of cm day^{-1} with three dimensionless factors that introduce variations into E. The first dimensionless factor is a diurnal demand function (Fig. **1b**) that produces a sinusoidal range from 0 to 1, representing the effects of both diurnal variations in air temperature on *VPD* and variations in stomatal aperture expected to result from diurnal light level changes. This diurnal function then multiplies a non-dimensional nominal *VPD* level (*nVPD*, 1 to 2.5) that represents maximum atmospheric sink strength, and a non-dimensional stomatal conductance (0 to 1) that captures the effect of leaf water stress on the realized evaporation rate (Fig. **1c**). The sigmoidal form of stomatal conductance as a function of leaf water potential is motivated by both typical field observations (Levin *et al.*, 2019) and direct hydromechanical experiments (Franks & Farquhar, 1999).

The dimensional potential transpiration rate, E_p, was set to a rate of 0.3 cm day^{-1} to match the intraday peak of 2 mmol m^{-2} s^{-1} seen in the heatwave experiment (Drake *et al.*, 2018; Fig. 2c). As a check on the appropriateness of the form of the diurnal function, total daily transpiration for the Control trees in that experiment was reported as approximately 1.5 kg m^{-2}, or ~ 1 mmol/day, which matches the peak rate of 2 mmol m^{-2} s^{-1} multiplied by 0.5, the value of the diurnal function integrated over a day, at an *nVPD* of 1. E_p is then defined as the peak transpiration rate observed for the control treatments, with the peak VPD for that treatment (~ 3 kpa) set to a nominal value of 1, and the (unreported) stomatal (or canopy) conductance associated with that peak rate

normalized to a value of one. E_p is then also akin to a dimensional maximum stomatal conductance, qualitatively similar to the reference stomatal conductance calculated by Novick *et al*. (2016) at low *VPD* for each quantile of soil moisture. The maximum flux from the water table J_m was then set to half of E_p, 0.15 cm day^{-1}. As the integral of the demand function over one day evaluates to 0.5, this choice of parameterization exactly balances the flux from the water table with total transpiration in the stress-free condition (no stomatal limitation) for an *nVPD* of 1 over the course of a day. For the Heat Wave treatment (*nVPD* 2), daily peak and total potential daily E_d for the Heat Wave treatment would be double that of the control, 0.6 cm day^{-1} and 0.3 cm day^{-1} respectively.

Given this model structure, the only possible source of a variable liquid phase resistance that could impose water stress in the leaf and so throttle stomatal conductance and *E* exists in the 10 cm soil domain between the lower maximum soil flux-fed boundary and upper root uptake plane. In this region changes in water content are related to changes in hydraulic conductivity and flux by Richard's equation (Fig. **1d**), neglecting gravitational effects over the 10 cm change in height. The governing equation, boundary conditions, and initial conditions are then linearized using the Kirchoff transform that allows expression of soil water content θ, soil matric potential h, and plant water potential Ψ in terms of a single variable for the potential flux in cm^2 day^{-1}, ζ (Supplemental Notes S1). One challenging feature of the resulting model is that the transformed stomatal conductance function falls sharply over a very small range of ζ (Fig. **1e**), complicating solution and introducing some numerical artifacts (discussed further in the results).

As the soil properties for the Heat Wave experiment were not reported, the hydraulic conductivity and matric potential functions of water content were parameterized based on Cowan (1965) for Yolo light clay. Initial soil water content in the model domain was then set to $\theta = 0.25$, or about half field capacity(Philip, 1957). To generate a range of behavior in the model, different ratios of potential daily evaporation (1/2 E_p x *nVPD*) to total daily soil flux (J_m) were investigated (note that the maximum soil flux J_m is equivalent to the total daily soil flux into the domain). In the first pair of model runs, a ratio of 1:1 was specified for the Control, and 2:1 for the Heat Wave, while for the second pair the Control ratio was set to 1.25:1 and the Heat Wave to 2.5:1. These four model runs then differed physically only in the ratio,

$$\frac{E_p \times nVPD}{2\,J_m}. \qquad eqn.1$$

Eqn 1 then represents the balance of actual source and *potential* sink flows integrated over a single day, and by construction (*i.e.*, the choice that E_p /2 balance J_m at *nVPD* 1) it is equivalent to *nVPD*. *nVPD* then provides a convenient descriptor for the differences in atmospheric aridity across the different model runs, but it is best thought of as a scaling factor for the balance of potential transpiration to soil water flux in *eqn* 1. Next, to test the effect of a reduction in the water potential for a 50% reduction in g_s Ψ50, a proxy for leaf osmotic adjustment, two additional model runs were compared with g_s Ψ50 set to -1.1 or -1.5 MPa, and *nVPD* set to 1.25 for both, with other parameters unchanged.

Finally, to initialize the transient model an arbitrary homogenous value of soil was specified for the model domain. The first three days of the model run then represent a transient period during which the initial uniform soil moisture decays to a persistent quasi-steady diurnally varying gradient, providing a four-day period comparable to the Heat Wave experiment over its duration. The models and figures were coded and evaluated in Mathematica 14 (Wolfram Inc., Champaign IL, USA; Supplemental Information Notes **S2**).

Results

Asymptotic finite soil flux in the limit of infinite driving force

In the absence of rainfall or irrigation, evaporation from the soil surface will lead to the establishment of a gradient in matric and gravitational potential from the surface to the water table (Jury et al., 1991). As soil hydraulic conductivity is itself a steep function of soil matric potential, over any finite distance from evaporative surface to the water table a finite flux emerges even as the matric potential of the evaporative surface goes to negative infinity (Supplemental Notes **S1**). Although Jury et al. (1991) approximate the resulting integral form relating the maximum flux to distance, the full solution for their fine sandy loam (Pachappa) and clay (Chino) soils (Fig. **2**) shows that the maximum flux of 0.15 cm day^{-1} used here as a boundary condition occurs for distance from the water table of 130 and 155 cm respectively. For the partial fit of Cowan (1965) over a range of soil moisture from θ = 0.25 to 0.1 to the data for Yolo clay (Philip 1957) used here to parameterize the soil hydraulic conductivity loss function,

the distance from water table to root uptake zone for the maximum flux of 0.15 cm day^{-1} specified in the model is predicted to be ~ 50 cm (Supplemental Information Fig. **S1**). In the physical experiment, based on the change in neutron counts for the soils beneath the trees of both control and HW treatments (Fig. **S2** in Drake *et al.*, 2018) the distance between the depth of greatest change in soil water content (50 cm) and no change in soil water content (150 cm) was one meter, a distance in the middle of the range of 50 and 150 cm predicted for the three soils considered here (Fig. **2**). Given this result, it seems reasonable to hypothesize that in the physical experiment soil properties and distance to the water table (*i.e.*, a location at which water content is fixed and therefore acts like a reservoir) imposed a maximum flux similar to 0.15 cm day^{-1}.

Applying the idea of a maximum flux that occurs in the limit of an infinitely dry surface may not make sense when the surface of interest can only achieve a finite level of dryness. The reason finite surfaces *might* approximate the infinite limit is that the relationship between maximum flux and driving force is a saturating function, such that each additional increment of tension pulling the water column toward the uptake surface results in ever diminishing increases in flux (Fig. **3**). For a soil surface in contact with air at 50% relative humidity, the surface-atmosphere local equilibrium water potential is almost -100 MPa, by which point the flux is certainly at its limit. Whether the limit holds for roots surfaces that are rarely drier than -1 MPa (Philip 1957) requires demonstration. Integrating the expression for maximum flux for Chino clay over finite ranges of water potential shows that the soil water flux is within 10% of the maximum at only -0.1 MPa, and 5% of the maximum by -0.2 MPa for distances from the water table to rooting plane up to a meter, with these values becoming more negative by 0.1 MPa as the distance grows to over two meters (Fig. **3**). Integration of soils for which the exponent $n = 3$ (e.g., Pachappa, Yolo) failed to converge over a finite range of potentials, but it seems reasonable to expect that soil water fluxes for most soils under drought are well approximated by the infinite limit.

Heat Wave: Recovery of intra- and inter-day patterns of transpiration under a doubling of VPD

The model successfully reproduced the patterns in *E* seen in the physical experiment across both the Contral and Heat Wave treatments (Figs. **4, 5**). For the Heat Wave treatment, the model captured both the phase shift of peak *E* to earlier in the AM and the steep decline in the PM relative to control (Figs. **4a, 5a**). At the daily time scale, the model also captured the re-charge of the system overnight, as shown by the re-opening of stomata to near maximum each morning,

as well as the conservation across both treatments of daily total *E* averaged over the four days of the experiment (Figs. **4a**, **5a** insets). Reproduction of the diurnal patterns of *E* suggests that the neglect of the radial geometry of the soil domain around individual roots did not prevent the development of sufficient soil hydraulic resistance to dry out modeled leaf water potential and reproduce the tight stomatal regulation seen in the physical experiment.

Not captured by the model was the tendency in the data of Drake *et al.* (2018) for the Heat Wave treatment to have a slightly higher daily peak transpiration rate. A higher morning peak *E* for the high *nVPD* treatment would be expected if an important reservoir of water *downstream* of the limiting liquid phase resistance was being emptied over the morning ramp up of *E*, and re-charging overnight. Given the lack of significant losses in leaf or stem hydraulics between the treatments reported by Drake *et al.*, (Supplemental Information, 2018), the limiting hydraulic resistance driving afternoon stomatal closure in the physical Heat Wave experiment must have occurred in the soil, and so variations in stored plant water (capacitance) could have driven the higher daily peaks of *E* seen in the Heat Wave treatment (Pfautsch *et al.*, 2015; McCarthy *et al.*, 2025). This means that more precise resolution of stomatal behavior at sub-daily time scales may require models that account for plant water storage.

Emergence of anisohydric and isohydric patterns of leaf water potential from the ratio of total atmospheric demand to maximum soil flux

Examination of the diurnal cycles of root and leaf water potentials (Fig **4b**, **5b**,) shows how aggressively soil loss of conductivity depresses root water potential across the various levels of *nVPD*. The control with *nVPD* 1 remained near 100% stomatal conductance, as the leaf water potential did not get dry enough to move stomatal conductance down the shoulder of its water potential curve (Fig. **4b**; Fig. **1c**). In the physical experiment, despite the doubling of *VPD* there was no definite pattern of differences in the mid-day leaf water potentials between treatments (Supplemental Information in Drake *et al.*, 2018), which together with significant reductions in mid-day *E* in the heat wave relative to the control fits the description of a strongly ‘isohydric’ response to *VPD*: ‘strict’ stomatal regulation holds mid-day leaf water potential at a near constant value (Hochberg *et al.*, 2018). For the treatment pairing of 1 and 2 *nVPD* for Control and Heat Wave respectively, although afternoon *E* followed an ‘isohydric’ pattern of strong mid-day curtailment of *E* in the Heat Wave, mid-day leaf water potentials across treatments showed a

characteristically ‘anisohydric’ response of falling from approximately -0.6 MPa to -1.5 MPa with higher evaporative demand. At the higher set of *nVPD*s of 1.25 and 2.5 for Control and Heat wave, the excess of daily E_p over the daily soil flux produced closer mid-day minimum leaf water potentials (~ -1.2 vs ~ -1.5 MPa) across both high and low *nVPD* treatments, a result more consistent with the apparent isohydry of the physical experiment. This suggests that for the low *VPD* Control treatment matching normal seasonal atmospheric conditions in the physical experiment, total evaporative demand already exceeded the maximum flux the droughted soil could provide.

Validation of the maximum soil flux boundary condition

Examining the model output for root water potentials provides a test of the appropriateness of the maximum soil flux boundary condition. At the lower *nVPD* 1 for the control, root water potentials oscillated between -0.1 and -0.2 MPa (Fig. **4b,** blue line), mild enough that the maximum flux concept may have overestimated the actual flux by as much as 10% at night and 5% during the day (Fig. **3**): if the flux had not been fixed at a maximum, root potentials would have had to dry down a further -0.1 MPa to pull a sufficient flux from the water table to balance total daily transpiration. Given that the further fall in stomatal conductance would have been imperceptibly small (Fig. **1c**), the modeled behavior of transpiration for the control treatment seems likely to be robust. For the Heat Wave treatment (Fig. **4b,** red line), the diurnal range of root water potentials between -0.2 and -1.6 MPa was sufficiently dry to closely approach the maximum flux limit, as were the other *nVPD* levels for both Control and Heat Wave (Fig. **5b**).

The behavior of integrated daily stomatal conductance as a proxy of assimilation

Given the conservation of daily E_d at the level of the control despite a doubling of *nVPD* in the Heat Wave treatment, intuitively one might expect that integrated stomatal conductance over the four-day Heat Wave treatment in the model would be depressed by half relative to the control. This was not the case in the model due to the diurnal cycle of soil water potential and stomatal responses being out of phase with the diurnal cycle of *nVPD*. Total aggregate demand (*nVPD* integrated over four days) did double from control to Heat Wave (2 vs 4), but integrated g_s over the four days for the Heat Wave was 75% to 66% Control (Fig. **4c**, **5c**, inset bar charts). Yet, in the physical experiment, carbon assimilation *A* for the Heat Wave treatment was about half that of the Control. This difference suggests that the experimental reduction in *A* for the Heat Wave

may have included non-stomatal effects, such as increased photorespiration, non-photochemical quenching, and thermal stress not modeled here. While g_s can follow a nearly linear relationship with assimilation in the ribulose bis-phosphate limited part of an a/c_i curve (Farquhar and Sharkey), purely hydraulic models are clearly inadequate for fully predicting carbon uptake and water use efficiency.

Response of daily integrated stomatal conductance and transpiration to osmotic adjustment in g_s $\Psi 50$

Departing from strict comparison to the Drake *et al.* (2018) experiment, the model was used to explore whether a hypothetical reduction in the g_s $\Psi 50$ for stomatal conductance from -1.1 MPa to -1.5 MPa for the trees in the Heat Wave treatment, as might occur due to osmotic adjustment shifting turgor loss and stomatal responses to more negative potentials, could rescue carbon uptake. Over the four-day model period, transpiration peaked at a slightly higher value after osmotic adjustment yet showed no important change when integrated over the four days (Fig. **6a**). As for both values of g_s $\Psi 50$ E was driven by the same *nVPD*, total g_s integrated over the four days would show the same lack of important difference as integrated daily E. In real plants, total daily carbon assimilation might be expected to benefit from the higher peaks in E and g_s at midday, due to lower CO_2 limitation and potentially lower leaf temperatures, effects not modeled here. Such potential marginal benefits to carbon balance aside, the simulations do show how the emergence of a maximum daily water budget from the fragility of hydraulic continuity in soils is likely to frustrate a strategy of attempting to maintain carbon fixation by tolerating more negative leaf water potentials.

VPD response of stomatal conductance with AM/PM hysteresis emerges from the balance of the total daily evaporative demand to the maximum soil flux

Plotting the instantaneous diurnal values for stomatal conductance and instantaneous *nVPD* (i.e., *nVPD* level multiplied by the diurnal function) results in an apparent stomatal response to variations in *nVPD* (Fig. 7). Fitting a *VPD* sensitivity model (Oren *et al*. 1999; Novick *et al.* 2016) of the form $g_s = g_{s,ref}\,(1- m \ln[nVPD])$ to these data results in a value of the slope parameter m of 0.786, well above the value of 0.65 proposed to indicate a dominant influence of *VPD* on canopy conductance (Novick *et al.*, 2016), and a $g_{s,ref}$ of 0.783. In this type of *VPD* sensitivity model, for each different quantile of bulk soil moisture $g_{s,ref}$ is fitted by definition at a *VPD* of 1

and m is fitted to the response of g_s as VPD increases: by construction, $g_{s,ref}$ is expected to capture all soil supply constraints on g_s, with m capturing the sensitivity of stomata to increasing atmospheric demand, generally interpreted as a species specific plant trait (Oren *et al.*, 1999). In the model presented here, the bulk soil moisture at the source-edge of the model domain is the same across all six simulations ($\zeta \sim 2$, $\theta \sim 0.28$, Supplemental Information Fig. **S2)**, fulfilling the definition of $g_{s,ref}$ in Fig. 7. Yet, in this SPAC model stomatal limitation emerges not simply from absolute VPD, but from the ratio of potential daily transpiration to the maximum flux available from the water table: $nVPD$ is equivalent to 0.5 E_p divided by J_m. The slope m fitted to the diurnal variations in $nVPD$ depends on the magnitude of atmospheric demand only in relation to the capacity of the soil to supply a given flux. Physically, this structure is stomatal sensitivity to VPD is to be expected if stomatal aperture is to ultimately (i.e., following any transient 'passive' wrong-way and 'active' ABA-mediated rectification; Brodribb & McAdam, 2011) constrain transpiration to not exceed the maximum flux available from the soil, as at steady-state it must.

Limitations and numerical artifacts

The steep non-linearity of the stomatal conductance function in the ζ domain (Fig. **1e**) did appear to introduce numerical artifacts in the model solution, most evident as jagged deviations from smooth curves (*e.g.*, Day 1 and 4 minimum g_s in Fig 4**c**). That such features are numerical artifacts could be confirmed by their vanishing for model runs with small variations in the initial conditions, as such variations would not be expected to make any difference in the behavior of the quasi-stationary state from day 3 to 7. However, such artifacts did constrain the range of stomatal Ψ50s relative to different ratios of total daily potential transpiration (0.5 E_p) and max soil flux J_m that could be explored, excluding very high and low values.

Discussion

Under what conditions is a maximum soil flux limiting?

The emergence of a maximum soil flux at relatively mild soil matric potentials can provide a sufficient explanation for the near perfect conservation of transpiration across a doubling of evaporative demand in the heat wave experiment. The question then arises of how representative that experiment may be for the behavior of other forested land surfaces. At the daily and sub-daily time scale, the highly stirred air in the whole tree chambers resulted in the convergence of

canopy and air temperatures, corresponding to natural cases for which a high canopy roughness and aerodynamic conductance, high wind speed, and turbulent mixing result in evaporation not being controlled by net radiation (Jarvis & McNaughton, 1986; McNaughton & Jarvis, 1991; McColl & Tang, 2024). At larger climatological temporal and spatial scales, atmospheric and soil moisture tend to be correlated as low water availability from the land surface dries out the atmosphere(Berg & Sheffield, 2018; Zhou *et al.*, 2019). Here we have shown that even over short time and spatial scales, the response of canopy conductance to *VPD* is inextricably linked to the dynamics of the capacity of the soil to supply the required transpiration flux. Yet, application of the maximum soil flux concept hinges on the availability of data on both plant rooting and water depths.

Over longer time scales, perennial plant rooting depth and soil water availability are not independent, and highly responsive to local soil conditions; as a result, plant species is a poor predictor of rooting depth (Fan *et al.*, 2017). Fan *et al.* (2017) describe how root growth follows infiltration depth, or the soil depth reached by the wetting front of meteoric water; if this depth is shallower than the capillary fringe of ground water, a ‘dry-gap’ is created between the rooting zone and deep soil moisture. Some trees obligately produce dimorphic roots, building both a shallow root system to access nutrients and seasonally available precipitation, as well as sending deep roots across the dry-gap to reach groundwater and avoid seasonal droughts(Skelton *et al.*, 2021). Yet most taxa remain dependent on meteoric water in the upper soil layers to support high transpiration rates. For 501 taxa, Fan *et al.* (2017) found maximum rooting depth clusters between ~25 cm and 2 m, with the highest density at 1m, paired with water table depths clustered between 1 and 10 m, creating the potential for meter scale dry gaps during drought for many, if not most, taxa.

How often might plants have to access water across such dry gaps? Miguez-Macho & Fan (2021)report that 70% global transpiration derives from the rain-fed upper soil layers, with moisture in deeper unsaturated soil and rocks accounting for 18%, locally recharged groundwater a mere 1%, and remotely (i.e., lateral flow) recharged groundwater 10%. The 11% due to groundwater seems likely to be due to dimorphic roots in the capillary fringe of the water table, for which the soil flux would be non-limiting. This leaves the 18% taken up from deep unsaturated as the fraction most likely to be governed by a maximum soil flux, though this

fraction may be higher in Mediterranean, semi-arid, and seasonally dry tropics (Miguez-Macho & Fan, 2021). By extension, instances of transpiration being limited by the maximum soil flux seem likely to be cases far from ecological equilibrium, such as drought, or in the case of species with dimorphic rooting strategies, during juvenile establishment phases in which the deep roots have not yet reached the capillary fringe. The Drake *et al.* (2018) experiment may fall into the latter category, as the experimental trees were young 6 m tall Eucalyptus that had been growing in soil for one year after being grown in pots to a size of 2 m. While Eucalyptus can grow dimorphic roots to depths in excess of 10 m, the neutron-probe measurements showed that for these young trees the largest changes in water content, presumably due to root uptake, occurred at a depth of only 50 cm. Under drought, plant survival depends on the balance of the minimum surface conductance, a combination of the degree of stomatal closure achieved and cuticular permeability, and the residual flux from the soil, which, in the presence of a water table at some depth, must ultimately converge with the maximum soil flux. It seems likely therefore that the concept of a maximum soil flux will have greater utility in understanding spatial and temporal patterns of plant survival under drought than in explaining patterns in transpiration across environments receiving varying precipitation (e.g., semi-arid versus mesic biomes).

Implications of a maximum soil flux for understanding plant traits responsive to drought

The emergence of a maximum flux is hardly unique to the case of 1D water flow from a water table to an evaporative surface. Such asymptotic behavior is a general feature of the continuum representation of flow through hydraulically vulnerable media, whether plant xylem (Sperry and Love 2015) or the soil (Cowan 1965; Carminati and Javaux 2020). As a result, both Sperry and Love (2015) and Carminati and Javaux (2020) define the desired ‘emergent’ behavior of stomata as down regulating E at the point where the curve of E versus canopy sap pressure/leaf water potential (the ‘supply function’) begins to saturate (i.e., becomes non-linear). Yet there is an important difference with respect to whether the limiting vulnerability is in the soil or plant xylem: the soil can simply ‘repair’ by rewetting and capillary action as the potential relaxes (thought there may be some hysteresis due to ‘ink bottle’ effects), while plant xylem once cavitated generally must be replaced with new growth. ‘Repair’ of plant xylem requires typically multiday periods of saturated soils and low to no evaporative demand, as gas bubbles must be compressed back into solution and then diffuse to the atmosphere (Lamarque *et al.*, 2018). As a

result, in large woody taxa most ecologically significant xylem refilling and repair occurs seasonally in spring following winter embolism in saturated soils prior to leaf out (e.g., Sperry et al., 1987). The difficulty of repair of xylem embolism then places a constraint on the precise point of stomatal regulation on the xylem supply function which does not exist for the soil. This simply means that with respect to the soil, stomata can err in targeting a point on the soil supply curve that is well past the onset of non-linearity without the direct penalty of permanent losses of conductivity. This can be seen in the test of the effect of making the water potential for 50% stomatal closure more negative (Fig. **6**): the soil simply forces leaf water potential to the value that limits transpiration to what the soil can sustain, without compromising the degree of hydraulic recovery overnight. Furthermore, the farther into the non-linear asymptotic part of the soil supply curve the stomata allow *E* to go, the tighter (more isohydric) the stomatal regulation when it finally occurs.

With respect to leaf traits enabling survival under drought, the aggressiveness of losses of soil conductivity puts the focus on the water potential at which stomata reach their minimum conductance (Hochberg *et al.*, 2018), rather than the water potential at which they begin to regulate. As long as the former potential is less negative than the stress causing embolism or cambial cell death, the plant has a chance to survive if the residual soil flux is greater than the residual transpiration rate of the plant, which may be reduced by leaf shedding (Sevanto *et al.*, 2014; Mantova *et al.*, 2023). Osmotic adjustment of leaf turgor loss and stomatal closure, as shown by the analysis in Fig. **6**, did not lead to an appreciable increase in total integrated g_s, a proxy for photosynthesis. However, it did appear to allow higher g_s during the initial model dry-down phase: this could mean there would be a benefit to osmotic adjustment under repeated cycles of partial rewetting that does not manifest under prolonged dry conditions. While turgor loss points (TLP) are correlated with dry conditions across taxa and biomes (Bartlett *et al.*, 2012), changes in root TLP and osmotic concentration across varieties with different reputations for drought performance can show complex patterns that may be confounded with deep and shallow rooting strategies (Bartlett *et al.*, 2022).

With respect to root traits, the models of Carminati and Javaux (2020) and Cowan (1965) demonstrate that traits promoting soil to root coupling, such as mucilage secretion, high root density, and high root to shoot ratio all serve to alleviate the fine scale gradients that occur

between the bulk soil and root surface for any combination of bulk soil water content and evaporative demand. However, this assessment is dependent on the steady-state boundary condition of a fixed soil moisture between each root-soil cylinder. For models with this structure, root-soil coupling emerges as a critical yet often difficult to resolve parameter that also determines whether the vulnerability of plant xylem or the soil provides the rate limiting vulnerability constraining transpiration (Sperry *et al.*, 1998). Applying a maximum soil flux as the boundary condition sidesteps this difficult question, as soil limitation emerges based on the macroscopic distance between maximum rooting depth and the water table, rather than the details of the rooting zone. This difference in sensitivities between models may be useful. Fitting both models with carefully parameterized soil data could reveal whether soil-root disconnection drives stomatal closure, or simply follows on after losses of soil conductivity have shut stomata.

Emergence of iso/aniso-hydric behavior

Previous work with simple SPAC models has shown that iso- and anisohydric behavior, the strict regulation of leaf water potential or lack thereof by stomatal conductance in response to declines in pre-dawn soil water potential and/or changes in *VPD*, is not a plant trait so much as a pattern that emerges from the interaction of plant and soil characteristics (Lhomme, 2001; Hochberg *et al.*, 2018). Typically in simplified SPAC models, the soil is treated as having a single potential that determines its hydraulic resistance, and a critical leaf water potential is defined that sets stomatal conductance to zero, as in Cowan (1965). This study shows, with a more realistic model of g_s, how a dynamic, intra-day drop in water potential at the root-soil interface, driven by the ratio of E_p to J_m, can switch the system from aniso- to isohydric behavior. Two refinements on the simpler analysis stand out. First, treating the soil as a continuous material (i.e., Cowan 1965) or series of discrete resistors (i.e., Sperry et al., 1998) rather than single ohmic resistor results in much tighter regulation of E due to the dynamic reduction in conductivity that is missing when a single Ohmic soil conductance depends on a fixed bulk soil potential. Second, under drought, site-to-site differences in the distance from rooting plane to water table and so J_m could cause the same genotypes under the same VPD and bulk soil moisture to show differences in iso/anisohydric behavior. While differences in root to water table distance should also theoretically affect pre-dawn bulk soil moisture in the rooting zone, the sensitivity is relatively small, at 100 Pa cm^{-1}. For example, increasing the distance from 50 to 100 cm shows a drop in J_m

from 0.78 cm/day to 0.24, a factor of 3, with only a decrease of 5 kPa in gravitational head and so equilibrium pre-dawn potential (Fig. **3**). Given the difficulty of resolving such small changes, it seem plausible that very different maximum soil fluxes, and so stomatal responses, could occur for apparently the same *VPD* and bulk soil matric potential.

Dynamic soil losses of conductivity confound modeled plant responses to VPD

The potential for different soil maximum fluxes, and so stomatal behavior, for the same bulk soil moisture and *VPD* has implications for models that define a reference value of g_s based on bulk soil moisture that is then modified by a slope parameter responsive to *VPD* (Oren *et al.*, 1999). In Novick *et al*. (2016), bulk soil moisture data, *VPD* and canopy conductances from Eddy flux towers were used to model canopy conductance as a function of *VPD* for different quantiles of soil moisture. From the perspective of the analysis presented here, bulk soil moisture is not a one-to-one function with maximum soil flux, and so cannot fully capture the influence of J_m on dynamic changes in soil conductivity. That in such *VPD* sensitivity models dynamic soil conductivity loss operates as a latent variable contributing to stomatal limitation calls into question the estimate that greater than 70% of surface conductance limitation in mesic forest biomes occurs in response to atmospheric dryness (Novick *et al.* 2016). Renormalizing *VPD* (or rather, potential transpiration) by a maximum soil flux could allow empirical models to better capture changes in the *VPD* response due to seasonal changes in the effective depth of water sources accessed by plants, potentially resulting in very different conclusions about the proportion of the land surface dominated by atmospheric demand.

Conclusion

Dynamic losses of soil conductivity can provide large diurnal potential drops capable of imposing a dominant constraint on transpiration rates. If unaccounted for, these dynamics can confound apparent stomatal responses to *VPD* as well as plant trait definitions. Yet, current modeling approaches that focus on the soil cylinder around a root are highly sensitive to assumptions about effective root length, and the related boundary condition of a fixed bulk soil water content at the outer margin of the model domain is likely to hold only at very low rooting volume. The neglect of the radial geometry of the flow around individual roots in favor of a 1D domain spanning the distance from a root ‘uptake plane’ to the water table offers the advantage of a well-defined water source and a parameterization that at certain time and spatial scales may

be simpler than estimating the appropriate measure of bulk soil moisture. Incorporation in the model of a realistic function for stomatal conductance comes at the cost of non-linearity and numerical instability, but successfully explains an experimental observation of conservation of total daily *E* over multiple days despite a doubling of *VPD*. This model suggests that the slope of apparent responses of stomatal conductance to *VPD* is controlled by the ratio of potential daily transpiration (0.5 E_p) to the maximum soil flux (J_m).

Acknowledgements

Abraham Stroock, Guido Salvucci, Kaighin McColl and N.M. Holbrook provided valuable feedback and discussion. This work was supported by NSF-MRSEC DMR-2011754.

Competing interests

None declared

Data availability

No new data were generated in this study, and all simulated data are available by evaluating the code given in Supplemental Information Notes **S2**.

Figure legends

Figure 1. Schematic of the model for the heat wave experiment. **a** The last ten centimeters of the distance *L* from the water table to rooting depth forms the explicitly modeled soil domain, bounded on the lower surface by a maximum flux from the water table J_m, and at the upper surface by a variable root uptake flux equivalent to transpiration *E* in response to diurnal demand (*nVPD*) in **b**. **c** Dimensionless stomatal conductance g_s as a function of leaf water potential Ψ [MPa], with the Ψ50 for a 50% decline in stomatal conductance set at -1.33 MPa (dotted lines). In the modeled domain **d**, water content θ depends on soil hydraulic conductivity that varies with the matric potential *K(h),* and the gradient in matric potential *h* [cm]. **e** Transformation of the water content, matric and water potentials to the potential flux domain [ζ, cm^2 day-1] helps linearize the governing equation, but at the cost of an extremely steep function for g_s that complicates solution.

Figure 2. Maximum fluxes [cm day^{-1}] for two soils parameterized by Jury *et al*. (1991). Although the saturated conductivities of the two soils differs six-fold, from 2 cm day^{-1} for the

clay soil to 12 cm day^{-1} for the more porous fine sandy loam, the maximum soil fluxes converge over longer distances from water table to rooting zone. The flux chosen to match the daily totals for transpiration in the experiment of Drake *et al.* (2018) of 0.15 cm day^{-1} occurs over 130 cm for the clay, and only 19% farther (over 155 cm) for the fine sandy loam (inset graphs with dotted lines).

Figure 3. Water flux in a Chino clay soil from a water table to an uptake surface (i.e., rooting plane) located a distance *L* above, as a function of the water potential of that surface (Ψ_{root}). As the root pulls with only 0.2 MPa of tension over moderate distances (50 and 100 cm), the flux approaches 95% (dotted vertical lines) of the asymptotic maximum fluxes (Fig. 2) for an infinite driving force. Over longer distances for *L* of 200 to 500 cm, the tension required to reach 95% increases to 0.3 MPa but remains modest.

Figure 4. Model results for the heat wave experiment in Drake *et al.* (2018) with normalized vapor pressure deficit (*nVPD)* levels of 1 (Control, blue lines) and 2 (Heat Wave, red lines). With this choice of *nVPDs*, the maximum soil flux equals 100% of the total daily potential evaporation for the control, and 50% for the heat wave. The first three days (shaded) represent a 'dry-down' from a SMC θ = 0.25 used to initialize the model to a four-day quasi-steady diurnal cycle comparable to the physical experiment. (**a**) Diurnal cycles of transpiration show the Heat Wave at *nVPD* 2 peaks earlier and shows steeper declines in afternoon *E* than the control at *nVPD* 1, but total daily *E* is conserved across both levels (inset bar chart). (**b**) Diurnal cycles of root (dashed line) and leaf (solid line) water potential Ψ at *nVPD* 1 are moderate, but at *nVPD* 2 root surface drying pushes leaf water potentials below -1 MPa in an apparent ‘anisohydric’ response to the difference in *nVPD*. (**c**) Diurnal variations in g_s show that the Control sees only minor stomatal limitation while the Heat Wave is forced to reduce g_s below 50% at midday: inset bar chart of integrated total g_s over four days, a proxy for carbon assimilation *A*, shows that, despite apparent anisohydry, *A* and *E* are strongly decoupled by higher *nVPD*.

Figure 5. Model results for the heat wave experiment in Drake *et al.* (2018) with normalized vapor pressure deficit (*nVPD)* levels of 1.25 (Control, blue lines) and 2.5 (Heat Wave, red lines): with this choice of *nVPD* s, the maximum soil flux is 80% (1/1.25) of total daily potential evaporation for the control, and 40% for the Heat Wave. The first three days (shaded) represent a 'dry-down' from a SMC of θ = 0.25 used to initialize the model to a four-day quasi-steady

diurnal cycle comparable to the physical experiment. (**a**) As before, diurnal cycles of transpiration show the Heat Wave peaks earlier and shows steeper declines in afternoon *E* than the Control, but total daily *E* is conserved across both levels (inset bar chart). (**b**) Diurnal variations in root (dashed line) and leaf (solid line) water potential show that for both values of *nVPD* root surface drying pushes leaf potential below -1 MPa, in an apparent near 'isohydric response' of Ψ_{leaf} to *nVPD*. (**c**) Diurnal variations in g_s show the development of stomatal limitation at midday in the control, but again total integrated g_s (as a proxy for *A*) and *E* are only strongly decoupled in the Heat Wave treatment.

Figure 6. Effect of an 'osmotic adjustment' shifting Ψ50 for g_s from -1.1 MPa (blue) to -1.5 MPa (black) on (a) diurnal transpiration and (b) diurnal g_s. Total daily E is conserved by the maximum soil flux across g_s Ψ50 levels (inset bar chart in a), and total daily g_s (inset in b), as a proxy for assimilation, shows that osmotic adjustment does not facilitate higher carbon gain.

Figure 7. Diurnal variations in VPD and stomatal conductance g_s over the four days compared to the physical heat wave experiment of Drake *et al.* (2018) for all four simulated dimensionless *nVPD* levels (cyan 1, green 1.25, red 2, blue 2.5), which represent the factors by which total daily potential transpiration (E_p /2, no stomatal limitation) equals (at *nVPD* 1) or exceeds (at *nVPD* > 1) the maximum soil flux from the water table. Black solid line shows the fit ($g_{s,ref}$ =0.783, m = 0.786) with and dashed lines the 99% CI (adjR^2 = 0.96) for the model g_s=$g_{s,ref}$ (1- m ln[*nVPD*]) over its applicable range of *nVPD* > 1(Oren et al., 2002; Novick et al 2016). Transient soil limitation of *E* results in the emergence of a phenomenological relationship between instantaneous values of *nVPD* and g_s.

References

Bartlett MK, Scoffoni C, Sack L. **2012**. The determinants of leaf turgor loss point and prediction of drought tolerance of species and biomes: A global meta-analysis. *Ecology Letters* **15**: 393–405.

Bartlett MK, Sinclair G, Fontanesi G, Knipfer T, Walker MA, McElrone AJ. **2022**. Root pressure-volume curve traits capture rootstock drought tolerance. *Annals of Botany* **129**: 389–402.

Berg A, Sheffield J. **2018**. Climate Change and Drought: the Soil Moisture Perspective. *Current Climate Change Reports* **4**: 180–191.

Brodribb TJ, McAdam SAM. **2011**. Passive origins of stomatal control in vascular plants. *Science* **331**: 582–585.

Buckley TN. **2005**. The control of stomata by water balance. *New Phytologist* **168**: 275–292.

Carminati A, Javaux M. **2020**. Soil Rather Than Xylem Vulnerability Controls Stomatal Response to Drought. *Trends in Plant Science* **25**: 868–880.

Carminati A, Vetterlein D, Weller U, Vogel H-J, Oswald SE. **2009**. When Roots Lose Contact. *Vadose Zone Journal* **8**: 805–809.

Carminati A, Zarebanadkouki M, Kroener E, Ahmed MA, Holz M. **2016**. Biophysical rhizosphere processes affecting root water uptake. *Annals of Botany* **118**: 561–571.

Cowan IR. **1965**. Transport of Water in the Soil-Plant-Atmosphere System. *Source: Journal of Applied Ecology* **2**: 221–239.

Dawson TE, Hahm WJ, Crutchfield-Peters K. **2020**. Digging deeper: what the critical zone perspective adds to the study of plant ecophysiology. *New Phytologist* **226**: 666–671.

Drake JE, Tjoelker MG, Vårhammar A, Medlyn BE, Reich PB, Leigh A, Pfautsch S, Blackman CJ, López R, Aspinwall MJ, *et al.* 2018. Trees tolerate an extreme heatwave via sustained transpirational cooling and increased leaf thermal tolerance. *Global Change Biology* **24**: 2390–2402.

Fan Y, Miguez-Macho G, Jobbágy EG, Jackson RB, Otero-Casal C. **2017**. Hydrologic regulation of plant rooting depth. *Proceedings of the National Academy of Sciences of the United States of America* **114**: 10572–10577.

Franks PJ, Farquhar GD. **1999**. Franks, Farquhar - 1999. : 1337–1349.

Hochberg U, Rockwell FE, Holbrook NM, Cochard H. **2018**. Iso/Anisohydry: A Plant–Environment Interaction Rather Than a Simple Hydraulic Trait. *Trends in Plant Science* **23**: 112–120.

Van Den Honert TH. **1948**. Water transport in plants as a catenary process. *Discussions of the Faraday Society* **3**: 146–153.

Jarvis P, McNaughton K. **1986**. Stomatal control of transpiration: Scaling up from leaf to region. In: MacFadyen A, Ford E, eds. Advances in Ecological Research. London: Academic Press, 1–45.

Javaux M, Carminati A. **2021**. Soil hydraulics affect the degree of isohydricity. *Plant Physiology* **186**: 1378–1381.

Jezek M, Blatt MR. **2017**. The membrane transport system of the guard cell and its integration for stomatal dynamics. *Plant Physiology* **174**: 487–519.

Jezek M, Hills A, Blatt MR, Lew VL. **2019**. A constraint–relaxation–recovery mechanism for stomatal dynamics. *Plant Cell and Environment* **42**: 2399–2410.

Jury WA, Gardner WR, Gardner WH. **1991**. *Soil Physics*. New York: Wiley.

Lamarque LJ, Corso D, Torres-Ruiz JM, Badel E, Brodribb TJ, Burlett R, Charrier G, Choat B, Cochard H, Gambetta GA, *et al.* 2018. An inconvenient truth about xylem resistance to embolism in the model species for refilling Laurus nobilis L. *Annals of Forest Science* **75**.

Levin AD, Williams LE, Matthews MA. **2019**. A continuum of stomatal responses to water deficits among 17 wine grape cultivars (Vitis vinifera). *Functional Plant Biology* **47**: 11–25.

Lhomme JP. **2001**. Stomatal control of transpiration: Examination of the Jarvis-type representation of canopy resistance in relation to humidity. *Water Resources Research* **37**: 689–699.

Manandhar A, Rimer IM, Soares Pereira T, Pichaco J, Rockwell FE, McAdam SAM. **2024**. Dynamic soil hydraulic resistance regulates stomata. *New Phytologist* **244**: 147–158.

Mantova M, Cochard H, Burlett R, Delzon S, King A, Rodriguez-Dominguez CM, Ahmed MA, Trueba S, Torres-Ruiz JM. **2023**. On the path from xylem hydraulic failure to downstream cell death. *New Phytologist* **237**: 793–806.

Matusick G, Ruthrof KX, Kala J, Brouwers NC, Breshears DD, Hardy GESJ. **2018**. Chronic historical drought legacy exacerbates tree mortality and crown dieback during acute heatwave-compounded drought. *Environmental Research Letters* **13**.

McAdam SAM, Brodribb TJ. **2016**. Linking turgor with ABA biosynthesis: Implications for stomatal responses to vapor pressure deficit across land plants. *Plant Physiology* **171**: 2008–2016.

McCarthy C, Bourbia I, Brodribb T. **2025**. Substantial capacitance found in the roots of 2 contrasting conifer species. *Plant Physiology* **198**.

McColl KA, Tang LI. **2024**. An Analytic Theory of Near-Surface Relative Humidity over Land. *Journal of Climate* **37**: 1213–1230.

McNaughton KG, Jarvis PG. **1991**. Effects of spatial scale on stomatal control of transpiration. *Agricultural and Forest Meteorology* **54**: 279–302.

Miguez-Macho G, Fan Y. **2021**. Spatiotemporal origin of soil water taken up by vegetation. *Nature* **598**: 624–628.

Mitchell PJ, O'Grady AP, Hayes KR, Pinkard EA. **2014**. Exposure of trees to drought-induced die-off is defined by a common climatic threshold across different vegetation types. *Ecology and Evolution* **4**: 1088–1101.

Novick KA, Ficklin DL, Stoy PC, Williams CA, Bohrer G, Oishi AC, Papuga SA, Blanken PD, Noormets A, Sulman BN, *et al.* 2016. The increasing importance of atmospheric demand for ecosystem water and carbon fluxes. *Nature Climate Change* **6**: 1023–1027.

Oren R, Sperry JS, Katul GG, Pataki DE, Ewers BE, Phillips N, Schäfer KVR. **1999**. Survey and synthesis of intra- and interspecific variation in stomatal sensitivity to vapour pressure deficit. *Plant, Cell and Environment* **22**: 1515–1526.

Parkhurst DF, Mott KA. **1990**. Intercellular diffusion limits to CO2 uptake in leaves: Studies in air and helox. *Plant Physiology* **94**: 1024–1032.

Pfautsch S, Hölttä T, Mencuccini M. **2015**. Hydraulic functioning of tree stems - Fusing ray anatomy, radial transfer and capacitance. *Tree Physiology* **35**: 706–722.

Philip J. **1957**. The Physical Principles of soil water movement during the irrigation cycle. In: Proceedings of 3rd International Commission on Irrigation and Drainage. 125–154.

Philip JR. **1966**. Plant water relations: some physical aspects. *Annual Review of Plant Biology* **17**: 245–268.

Roderick ML, Greve P, Farquhar GD. **2015**. On the assessment of aridity with changes in atmospheric CO2. *Water Resources Research* **51**: 5450–5463.

Rodriguez-Dominguez CM, Brodribb TJ. **2020**. Declining root water transport drives stomatal closure in olive under moderate water stress. *New Phytologist* **225**: 126–134.

Sevanto S, Mcdowell NG, Dickman LT, Pangle R, Pockman WT. **2014**. How do trees die? A test of the hydraulic failure and carbon starvation hypotheses. *Plant, Cell and Environment* **37**: 153–161.

Skelton RP, Anderegg LDL, Diaz J, Kling MM, Papper P, Lamarque LJ, Delzon S, Dawson TE, Ackerly DD. **2021**. Evolutionary relationships between drought-related traits and climate shape large hydraulic safety margins in western North American oaks. *Proceedings of the National Academy of Sciences of the United States of America* **118**.

Sperry JS, Adler F, Campbell G, Comstock J. **1998**. Limitation of plant water use by rhizosphere and xylem conductance: results from a model. *Plant, Cell and Environment* **21**: 347–359.

Sperry JS, Holbrook NM, Zimmermann MH, Tyree MT. **1987**. Spring Filling of Xylem Vessels in Wild Grapevine. *Plant Physiology* **83**: 414–417.

Sperry JS, Love DM. **2015**. What plant hydraulics can tell us about responses to climate-change droughts. *New Phytologist* **207**: 14–27.

Tardieu F, Simonneau T. **1998**. Taradieu, modelling isohydric and anisohydric behaviours JXB 1998.pdf. *Journal of Experimental Botany* **49**: 419–432.

Torres-Ruiz JM, Jansen S, Choat B, McElrone AJ, Cochard H, Brodribb TJ, Badel E, Burlett R, Bouche PS, Brodersen CR, *et al.* 2015. Direct X-ray microtomography observation confirms the induction of embolism upon xylem cutting under tension. *Plant Physiology* **167**: 40–43.

Wheeler JKJK, Huggett BABA, Tofte ANAN, Rockwell FEFE, Holbrook NMM. **2013**. Cutting xylem under tension or supersaturated with gas can generate PLC and the appearance of rapid recovery from embolism. *Plant, Cell and Environment* **36**: 1938–1949.

Zhou S, Park Williams A, Berg AM, Cook BI, Zhang Y, Hagemann S, Lorenz R, Seneviratne SI, Gentine P. **2019**. Land–atmosphere feedbacks exacerbate concurrent soil drought and atmospheric aridity. *Proceedings of the National Academy of Sciences of the United States of America* **116**: 18848–18853.

Supplemental Information

Notes **S1**. Derivation of a maximum soil flux and the governing equation.

Notes **S2**. Computer code for the model and figures.

Fig. **S3.** Maximum soil flux for the soil parameterization used in the model.

Fig. **S4**. Evolution of the potential flux ζ for all levels of *nVPD* over the course of the seven-day simulation.

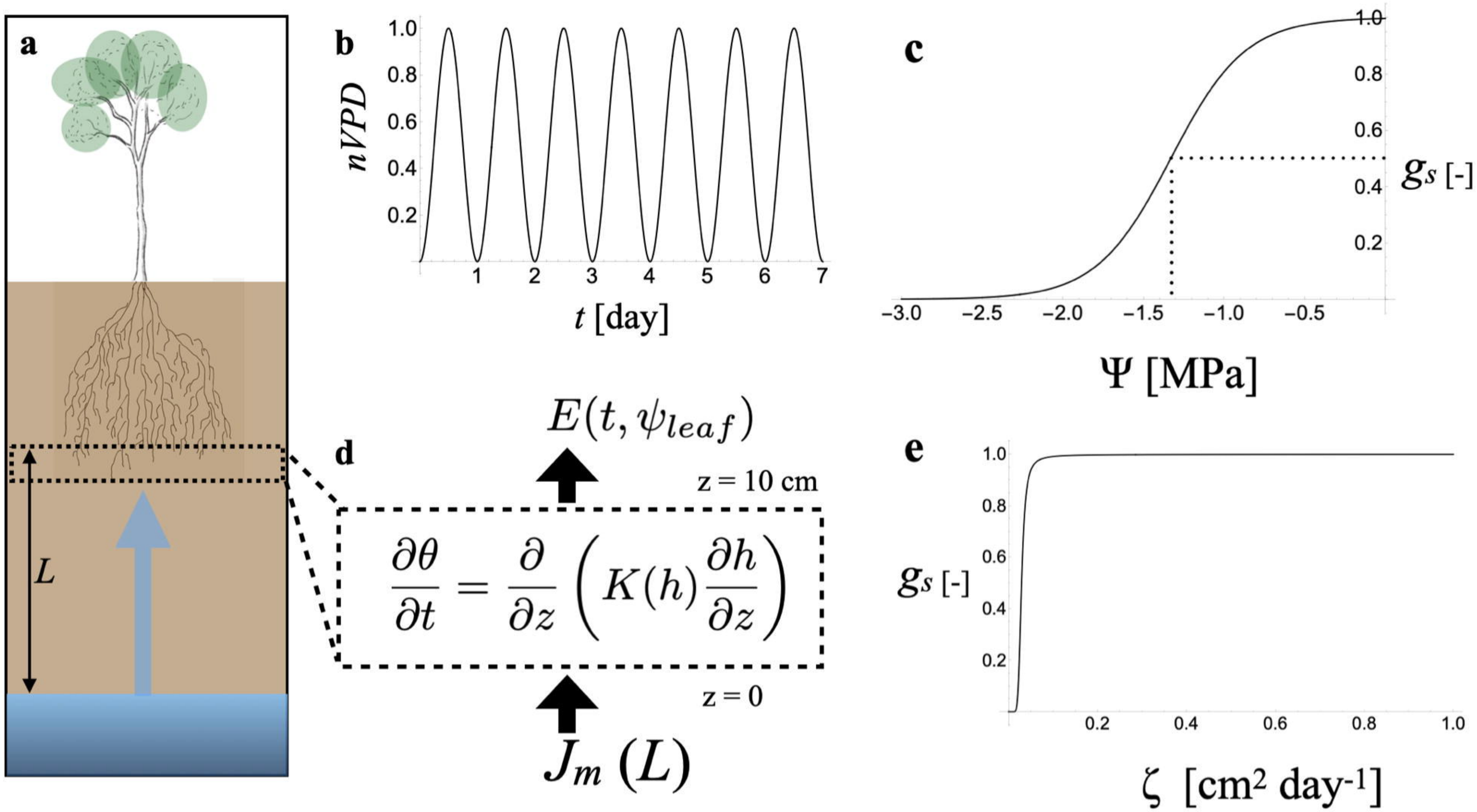

Figure 1. Schematic of the model for the heat wave experiment. **a** The last ten centimeters of the distance L from the water table to rooting depth forms the explicitly modeled soil domain, bounded on the lower surface by a maximum flux from the water table J_m, and at the upper surface by a variable root uptake flux equivalent to transpiration E in response to diurnal demand (*nVPD*) in **b**. **c** Dimensionless stomatal conductance g_s as a function of leaf water potential Ψ [MPa], with the Ψ50 for a 50% decline in stomatal conductance set at -1.33 MPa (dotted lines). In the modeled domain **d**, water content θ depends on soil hydraulic conductivity that varies with the matric potential *K(h),* and the gradient in matric potential h [cm]. **e** Transformation of the water content, matric and water potentials to the potential flux domain [ζ, cm^2 day-1] helps linearize the governing equation, but at the cost of an extremely steep function for g_s that complicates solution.

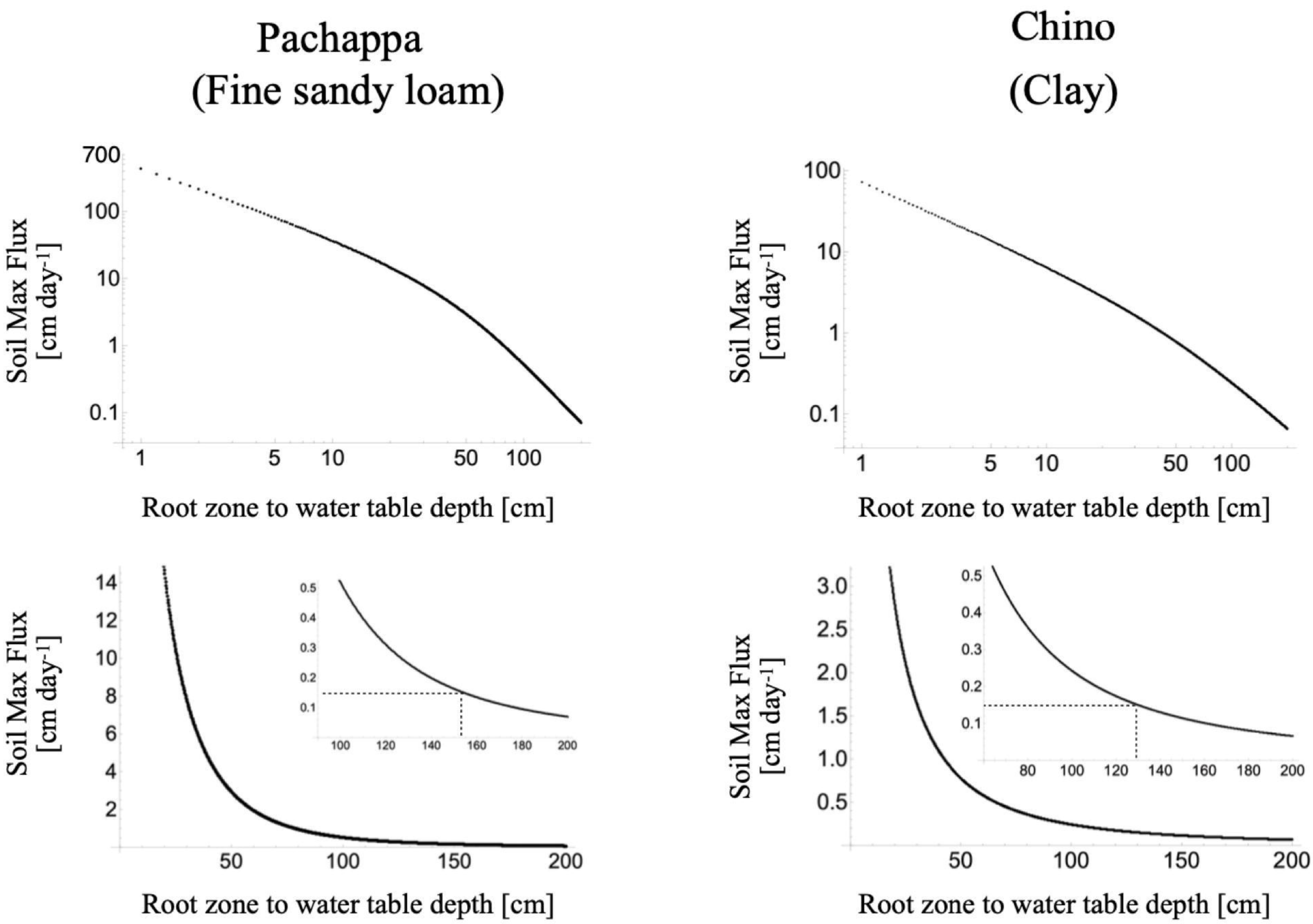

Figure 2. Maximum fluxes [cm day^{-1}] for two soils parameterized by Jury *et al.* (1991). Although the saturated conductivities of the two soils differs six-fold, from 2 cm day^{-1} for the clay soil to 12 cm day^{-1} for the more porous fine sandy loam, the maximum soil fluxes converge over longer distances from water table to rooting zone. The flux chosen to match the daily totals for transpiration in the experiment of Drake *et al.* (2018) of 0.15 cm day^{-1} occurs over 130 cm for the clay, and only 19% farther (over 155 cm) for the fine sandy loam (inset graphs with dotted lines).

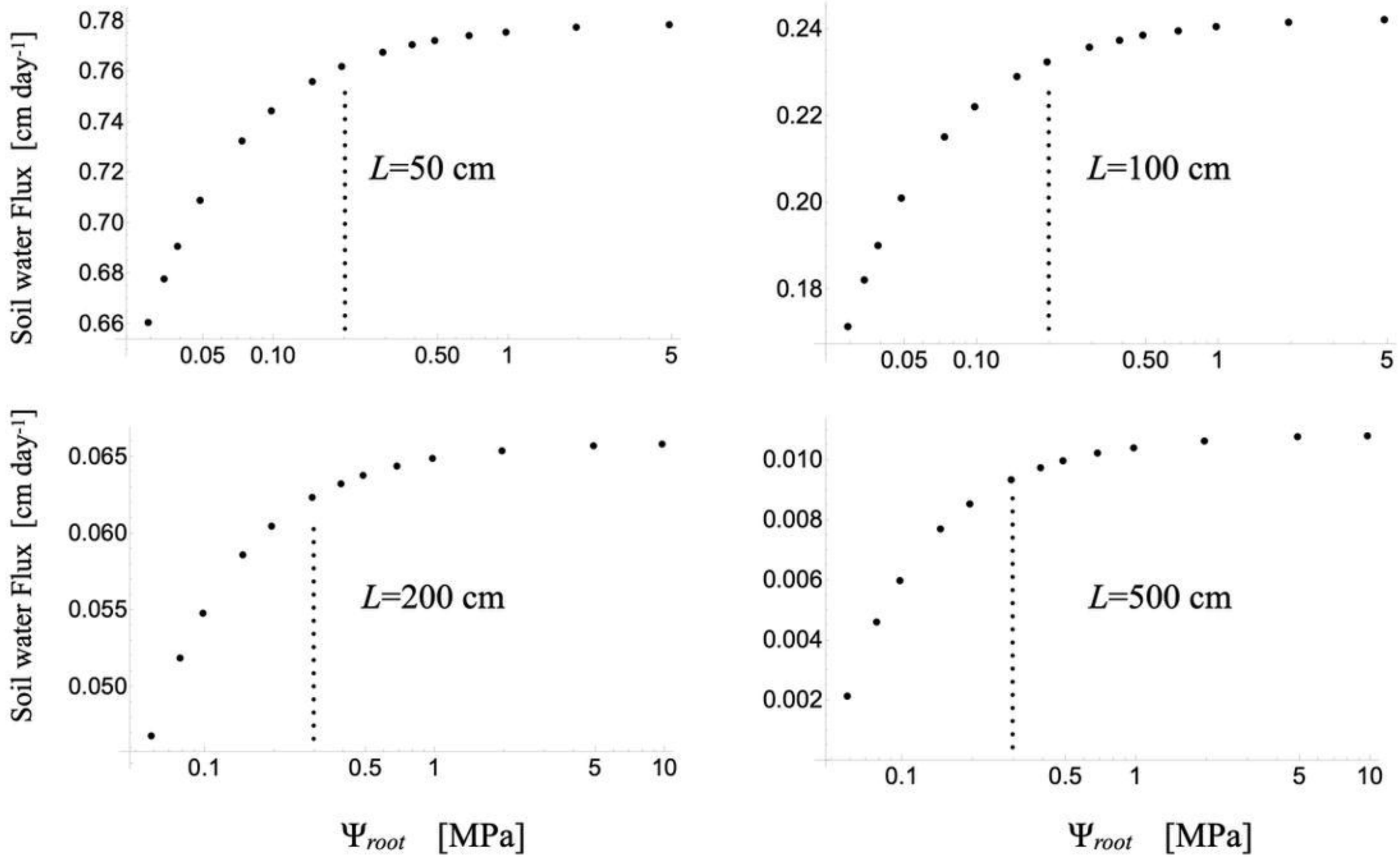

Figure 3. Water flux in a Chino clay soil from a water table to an uptake surface (i.e., rooting plane) located a distance L above, as a function of the water potential of that surface (Ψ_{root}). As the root pulls with only 0.2 MPa of tension over moderate distances (50 and 100 cm), the flux approaches 95% (dotted vertical lines) of the asymptotic maximum fluxes (Fig. 2) for an infinite driving force. Over longer distances for L of 200 to 500 cm, the tension required to reach 95% increases to 0.3 MPa but remains modest.

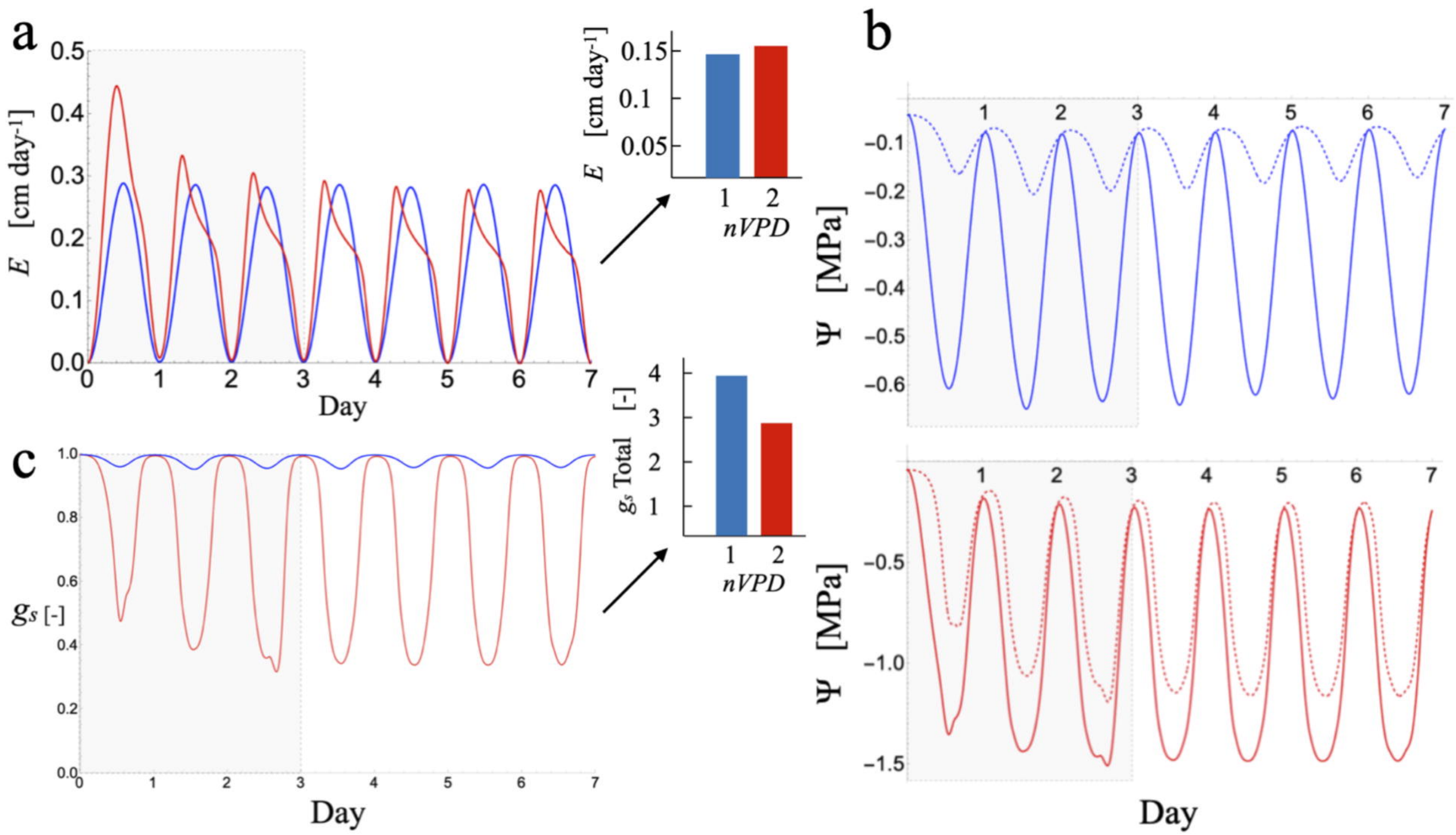

Figure 4. Model results for the heat wave experiment in Drake *et al.* (2018) with normalized vapor pressure deficit (*nVPD)* levels of 1 (Control, blue lines) and 2 (Heat Wave, red lines). With this choice of *nVPDs*, the maximum soil flux equals 100% of the total daily potential evaporation for the control, and 50% for the heat wave. The first three days (shaded) represent a 'dry-down' from a SMC $\theta = 0.25$ used to initialize the model to a four-day quasi-steady diurnal cycle comparable to the physical experiment. (**a**) Diurnal cycles of transpiration show the Heat Wave at *nVPD* 2 peaks earlier and shows steeper declines in afternoon *E* than the control at *nVPD* 1, but total daily *E* is conserved across both levels (inset bar chart). (**b**) Diurnal cycles of root (dashed line) and leaf (solid line) water potential Ψ at *nVPD* 1 are moderate, but at *nVPD* 2 root surface drying pushes leaf water potentials below -1 MPa in an apparent 'anisohydric' response to the difference in *nVPD*. (**c**) Diurnal variations in g_s show that the Control sees only minor stomatal limitation while the Heat Wave is forced to reduce g_s below 50% at midday: inset bar chart of integrated total g_s over four days, a proxy for carbon assimilation *A,* shows that, despite apparent anisohydry, *A* and *E* are strongly decoupled by higher *nVPD*.

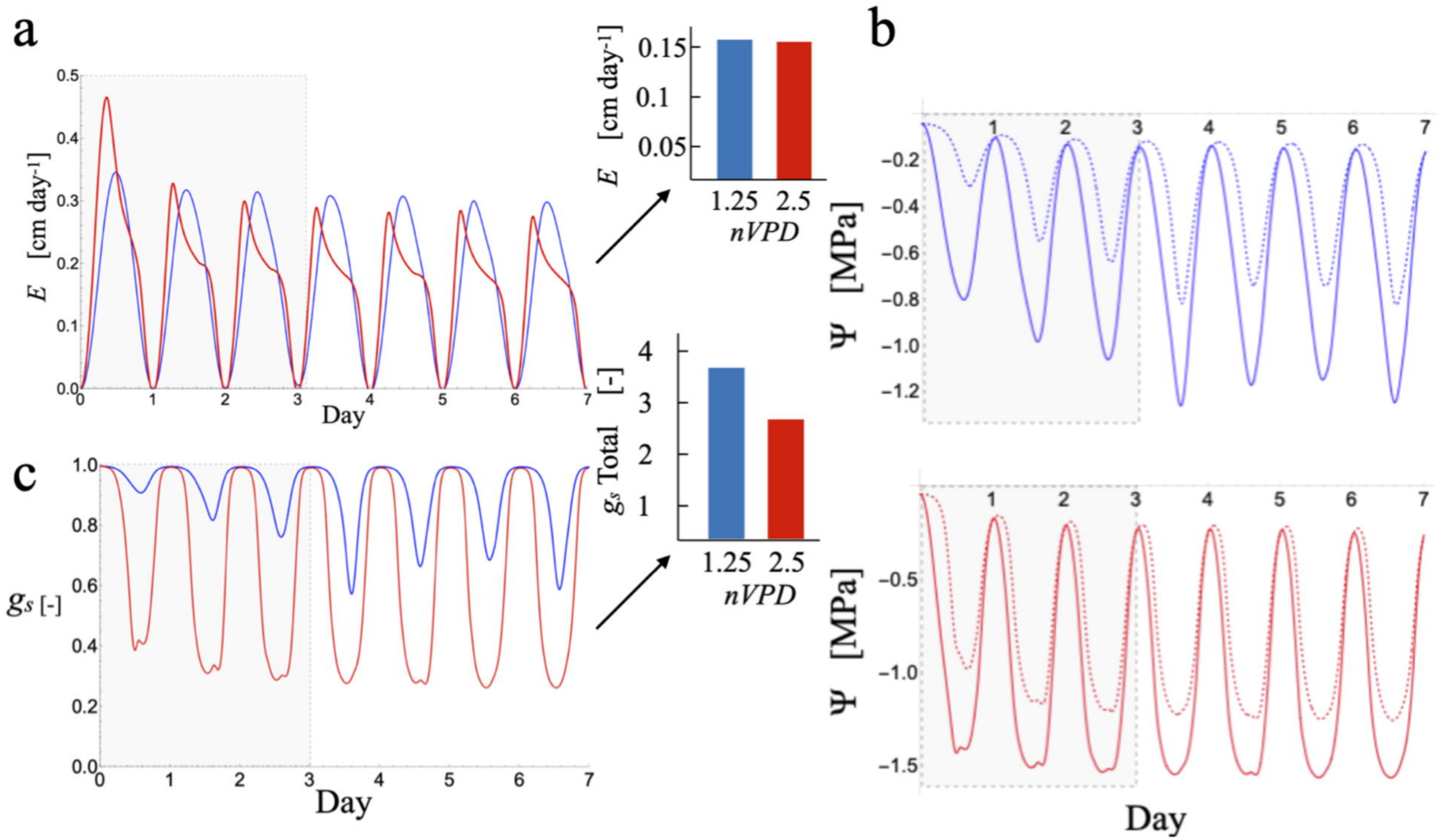

Figure 5. Model results for the heat wave experiment in Drake *et al.* (2018) with normalized vapor pressure deficit (*nVPD)* levels of 1.25 (Control, blue lines) and 2.5 (Heat Wave, red lines): with this choice of *nVPD* s, the maximum soil flux is 80% (1/1.25) of total daily potential evaporation for the control, and 40% for the Heat Wave. The first three days (shaded) represent a 'dry-down' from a SMC of $\theta = 0.25$ used to initialize the model to a four-day quasi-steady diurnal cycle comparable to the physical experiment. (**a**) As before, diurnal cycles of transpiration show the Heat Wave peaks earlier and shows steeper declines in afternoon *E* than the Control, but total daily *E* is conserved across both levels (inset bar chart). (**b**) Diurnal variations in root (dashed line) and leaf (solid line) water potential show that for both values of *nVPD* root surface drying pushes leaf potential below -1 MPa, in an apparent near 'isohydric response' of Ψ_{leaf} to *nVPD*. (**c**) Diurnal variations in g_s show the development of stomatal limitation at midday in the control, but again total integrated g_s (as a proxy for *A*) and *E* are only strongly decoupled in the Heat Wave treatment.

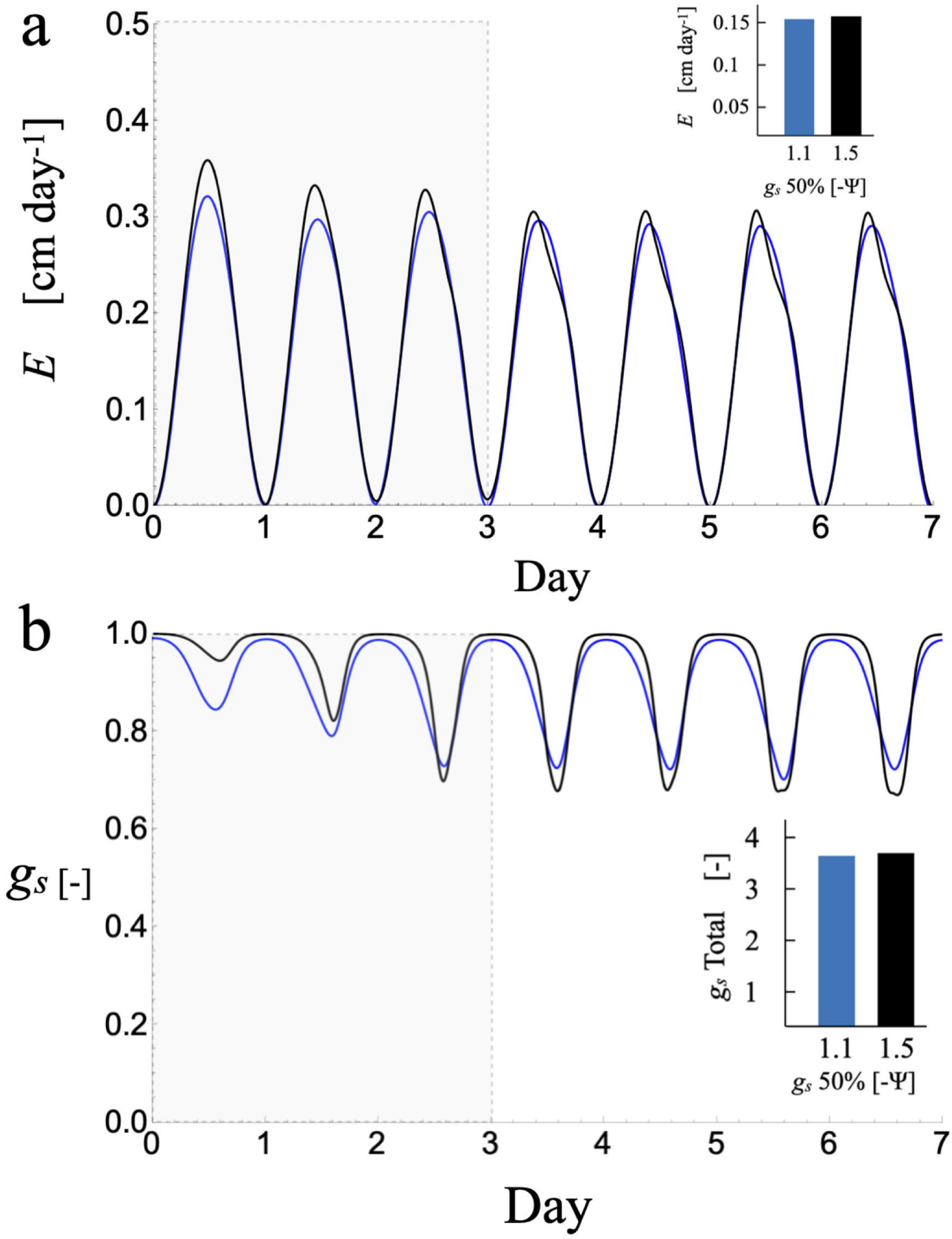

Figure 6. Effect of an 'osmotic adjustment' shifting Ψ50 for g_s from -1.1 MPa (blue) to -1.5 MPa (black) on (a) diurnal transpiration and (b) diurnal g_s. Total daily E is conserved by the maximum soil flux across g_s Ψ50 levels (inset bar chart in a), and total daily g_s (inset in b), as a proxy for assimilation, shows that osmotic adjustment does not facilitate higher carbon gain.

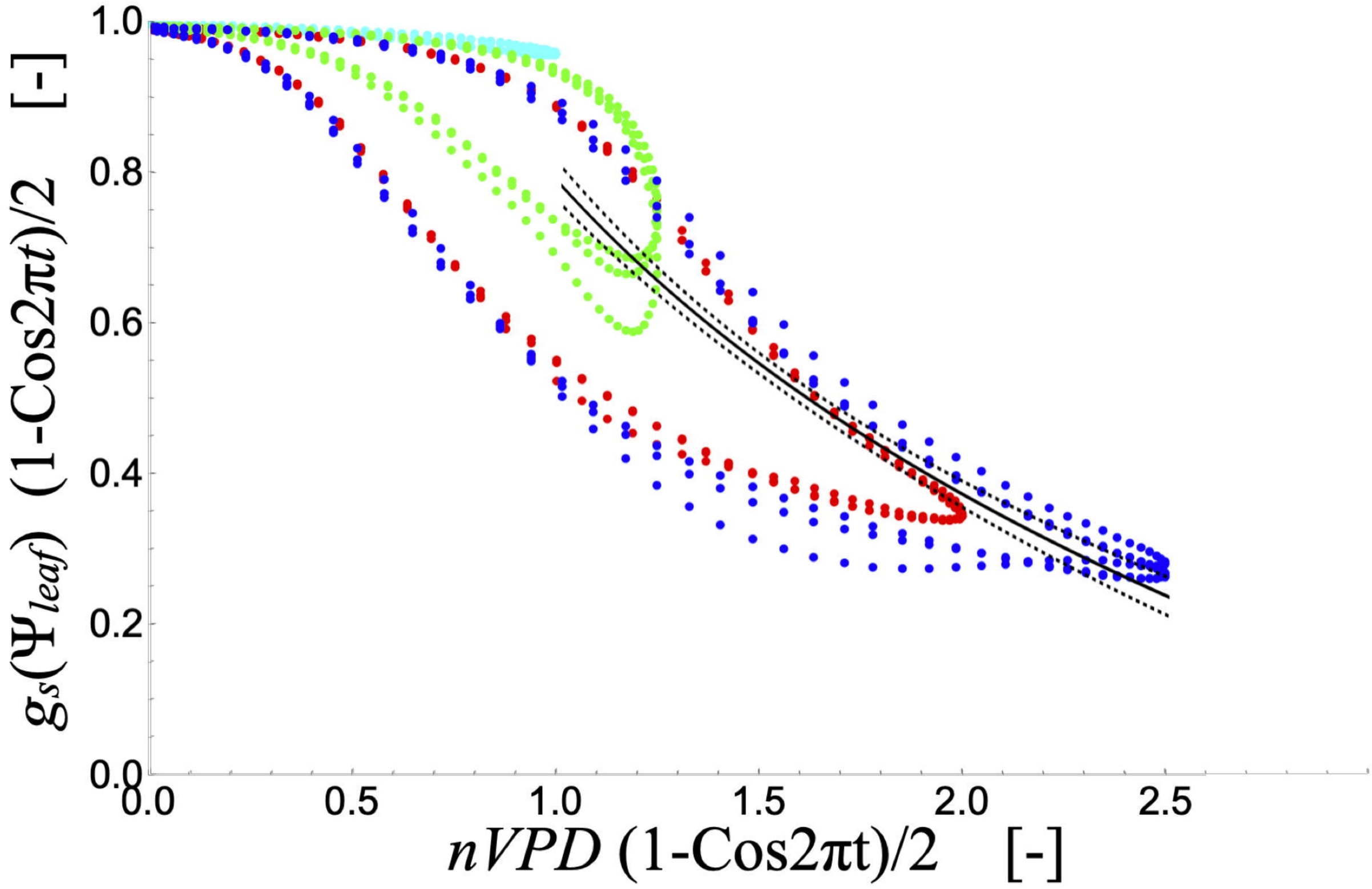

Figure 7. Diurnal variations in VPD and stomatal conductance g_s over the four days compared to the physical heat wave experiment of Drake *et al.* (2018) for all four simulated dimensionless *nVPD* levels (cyan 1, green 1.25, red 2, blue 2.5), which represent the factors by which total daily potential transpiration (E_p /2, no stomatal limitation) equals (at *nVPD* 1) or exceeds (at *nVPD* > 1) the maximum soil flux from the water table. Black solid line shows the fit ($g_{s,ref}$ =0.783, m = 0.786) with and dashed lines the 99% CI (adjR^2 = 0.96) for the model g_s=$g_{s,ref}$ (1- m ln[*nVPD*]) over its applicable range of *nVPD* > 1(Oren et al., 2002; Novick et al 2016). Transient soil limitation of *E* results in the emergence of a phenomenological relationship between instantaneous values of *nVPD* and g_s.